Characterizing the Cytocompatibility of Various Cross-Linking Chemistries for the Production of Biostable Large-Pore Protein Crystal Materials

Luke F. Hartje,[1] Hieu T. Bui,[2] David A. Andales,[3] Susan P. James,[2,4] Thaddaus R. Huber,[3] and Christopher D. Snow*[1,2,3]

Department of Biochemistry and Molecular Biology,[1] School of Biomedical Engineering,[2] Department of Chemical and Biological Engineering[3] and Department of Mechanical Engineering[4] Colorado State University, Fort Collins, CO 80521, USA

KEYWORDS: protein crystal engineering, biocompatibility, stability, toxicity, nanotechnology, nanoporous material, porous scaffold

ABSTRACT: With rapidly growing interest in therapeutic macromolecules, targeted drug delivery, and *in vivo* biosensing comes the need for new nanostructured biomaterials capable of macromolecule storage and metered release that exhibit robust stability and cytocompatibility. One novel possibility for such a material are engineered large-pore protein crystals (LPCs). Here, various chemically-stabilized LPC derived biomaterials were generated using three cross-linking agents: glutaraldehyde, oxaldehyde, and 1-Ethyl-3-(3-dimethylaminopropyl)carbodiimide. LPC biostability and *in vitro* mammalian cytocompatibility was subsequently evaluated and compared to similarly cross-linked tetragonal hen egg white lysozyme crystals. This study demonstrates the ability of various cross-linking chemistries to physically stabilize the molecular structure of LPC materials—increasing their tolerance to challenging conditions while exhibiting minimal cytotoxicity. This approach produces LPC derived biomaterials with promising utility for diverse applications in biotechnology and nanomedicine.

Protein crystals, typically evaluated solely for the elucidation of three-dimensional protein structure through X-ray diffraction, have unique chemical and material qualities—most notably, their self-assembling, homochiral, highly-ordered nanoporous structure. Intriguingly, the chemical properties of protein crystal materials can be readily engineered through genetic or chemical modification of their monomeric protein constituents. A common example of protein crystal modification involves the introduction of covalent bonds between adjacent monomers using bifunctional reagents.[1] This chemical cross-linking has been shown to greatly improve overall crystal stability,[2–4] thereby broadening the potential for protein crystals to be used in diverse material applications.[5]

One distinct advantage of protein crystals over chemically synthesized nanoporous scaffolds, such as zeolites and metal organic frameworks, is their biological origin; biologically derived nanoporous materials have been recognized as attractive scaffolds for applications in which biodegradability and/or biocompatibility is preferred. Some of these applications include: drug delivery,[6,7] vaccinations,[8] environmental remediation,[9] and biosensing.[10–12] However, stabilizing biologically derived materials with chemical cross-linkers can lead to increases in cytotoxicity.[13–15] Despite this risk, we are unaware of any studies that have quantified the cytotoxicity and stability of various chemically cross-linked protein crystal materials. Therefore, the extent of any toxic effects the cross-linking process may impart to protein crystal materials is unclear, nor is it clear whether the nanostructure of these biomaterials can survive in contact with living cells or tissues.

To demonstrate the feasibility of utilizing chemically-stabilized protein crystal materials in biological and environmental applications in which both toxicity and material stability is a concern, we investigated the efficacy of various cross-linking reagents to stabilize the molecular structure of two distinct protein crystal variants while minimizing cytotoxicity. The first crystal variant used in this study is a large-pore protein crystal (LPC) composed of CJ monomers (Fig. 1A & 1C). CJ is a modified form of a putative periplasmic isoprenoid binding protein derived from *Campylobac-*

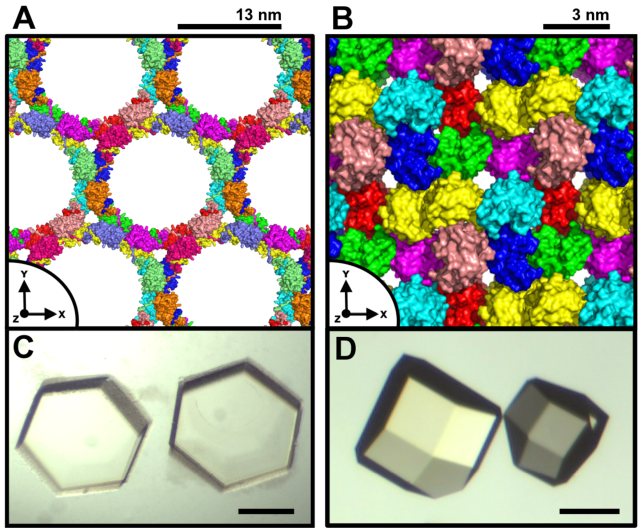

Figure 1. (A) CJ-LPC crystal lattice (PDB: 5W17) showing large (13 nm) pores. (B) Tetragonal HEWL crystal lattice (PDB: 2HTX) showing much smaller and more typical pore sizes (<2 nm). (C) CJ-LPCs in growth well. *Scale bar*: 200 µm. (D) HEWL crystals in growth well. *Scale bar*: 100 µm.

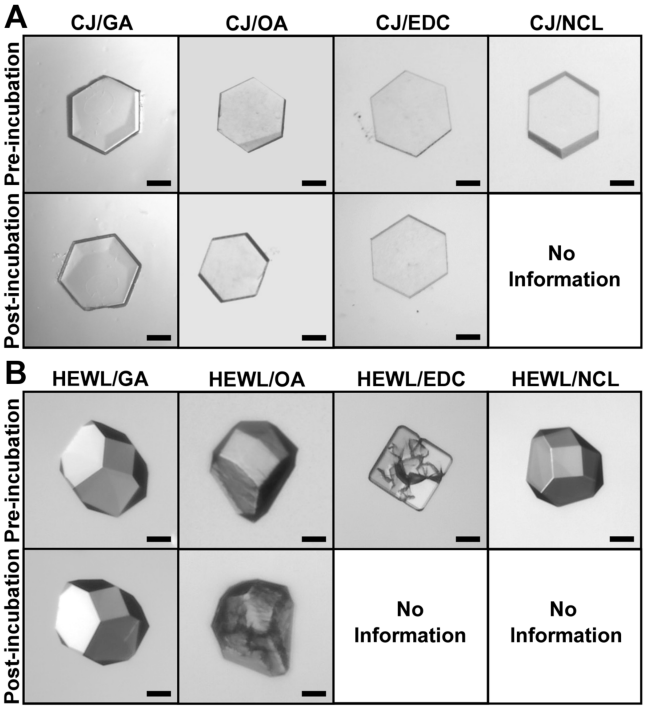

Figure 2. Stereomicroscopy images of protein crystals taken both before (*pre-incubation*) and after (*post-incubation*) 24-hour incubation with HDFa cells. (A) CJ-LPCs; *Scale bar*: 100 μm. (B) HEWL crystals; *Scale bar*: 50 μm. Note: 'No Information' indicates the crystals dissolved during

ter jejuni. Our lab has shown that CJ derived large-pore protein crystals (CJ-LPCs) have properties uniquely suited for programmable organization of macromolecular guests at distinct sites within hundreds of millions of precisely defined pores.[16–18] The combination of high theoretical capacity for guest macromolecules and the mechanical strength of a cross-linked honeycomb lattice make CJ-LPCs attractive molecular depots for use in various biomedical and environmental applications. As a point of comparison, the second crystal variant studied was tetragonal hen egg white lysozyme (HEWL), which represents a more comprehensively studied protein crystal system with archetypal pore sizes (Fig. 1B & 1D).

Large (100–500 μm diameter) CJ-LPCs were grown by sitting drop vapor diffusion at 20° C in 3.3–3.6 M $(NH_4)_2SO_4$, 100 mM bis-tris at pH 7.0 (Fig. 1C). Tetragonal HEWL crystals were grown per a modified version of a previously described batch crystallization protocol[19] (Fig. 1D). Prior to cross-linking, crystals were washed in buffered high-salt solutions to remove residual protein monomers without compromising the integrity of the crystal. Washed crystals were then cross-linked by direct addition of one of three chemical cross-linkers: 1-Ethyl-3-(3-dimethylaminopropyl)carbodiimide (EDC), glutaraldehyde (GA), or oxaldehyde (OA) to introduce covalent attachments between adjacent monomers, thereby generating various chemically stabilized protein crystal materials. In all cases, cross-linking was performed in solutions intended to mimic the mother liquor to mitigate crystal degradation. Protein expression, purification, crystallization, and cross-linking are described in more detail in the Supporting Information.

The efficacy of various cross-linking chemistries in stabilizing protein crystals on a macroscopic level was investigated using stereomicroscopy. Images were taken of crystals in high-salt conditions directly after cross-linking (*pre-incubation*) and again after 24-hour incubation with adult human dermal fibroblast (HDFa) cells at 37° C (*post-incubation*). Pre-incubation images of cross-linked CJ-LPC materials (CJ/GA, CJ/OA, CJ/EDC) demonstrate similar macroscopic crystal quality as the washed non-cross-linked CJ-LPCs (CJ/NCL) (Fig. 2A *pre-incubation*), thus indicating these cross-linking methods do not overtly lead to CJ-LPC deterioration. As expected, the comparatively low salt and high temperature environment associated with HDFa cell culture caused CJ/NCL crystals to completely dissolve within 24-hours. Conversely, all chemically stabilized CJ-LPCs continued to show no loss of crystal quality despite being transferred away from their high-salt crystallization environment (Fig. 2A *post-incubation*). Therefore, all three cross-linking chemistries are shown to be independently sufficient and necessary to preserve the short-term macroscopic structure of CJ-LPCs in the presence of living cells. Complementary images of cross-linked HEWL crystals taken prior to incubation with HDFa cells reveal HEWL/GA crystals to have similar quality as the washed HEWL/NCL crystals; however, images of HEWL/OA and HEWL/EDC crystals show moderate to severe surface deformation and cracking (Fig. 2B *pre-incubation*). Post-incubation images of HEWL/GA crystals continue to evince no loss of crystal quality while images of HEWL/OA reveal increased cracking and severe crystal deterioration—HEWL/EDC and HEWL/NCL crystals completely dissolved (Fig. 2B *post-incubation*). These results suggest that the cross-linking methods for HEWL/EDC and HEWL/OA were not sufficient to stabilize the macro-

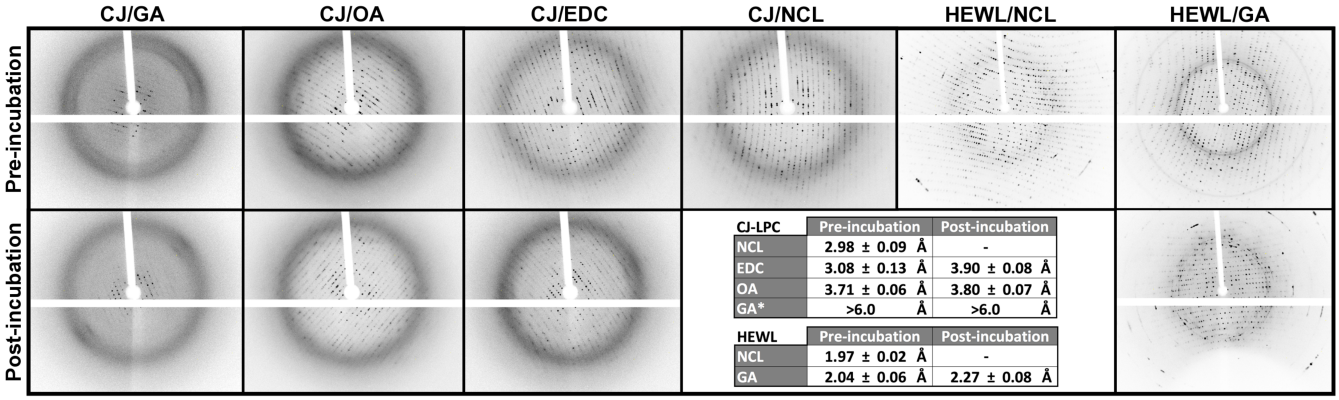

CJ-LPC	Pre-incubation	Post-incubation
NCL	2.98 ± 0.09 Å	-
EDC	3.08 ± 0.13 Å	3.90 ± 0.08 Å
OA	3.71 ± 0.06 Å	3.80 ± 0.07 Å
GA*	>6.0 Å	>6.0 Å

HEWL	Pre-incubation	Post-incubation
NCL	1.97 ± 0.02 Å	-
GA	2.04 ± 0.06 Å	2.27 ± 0.08 Å

Figure 3. Representative XRD diffraction patterns both pre- and post-incubation with HDF cells. *Tables:* High-resolution estimates for each diffraction set. See Supporting Information for XRD replicate data and resolution estimate details. *Note:* there is no resolution estimate for post-incubation NCL crystals due to the crystals dissolving when transferred outside their respective crystallization conditions. *The high-resolution estimate (>6.0 Å) for CJ/GA crystals is a qualitative estimate based on observable spots—the reflection data could not be comparatively indexed and scaled due to poor diffraction.

scopic structure of tetragonal HEWL, resulting in severe crystal degradation and/or disintegration.

To further examine cross-linked crystal stability, the molecular order of sufficiently cross-linked protein crystal materials (CJ/GA, CJ/OA, CJ/EDC, HEWL/GA) was analyzed both pre- and post-incubation with HDFa cells by X-ray diffraction (XRD) on a Rigaku HomeLab (Fig 3). Pre-incubation CJ/OA and CJ/EDC crystals achieved diffraction out to approximately 3.7 and 3.1 Å respectively, which is comparable to the washed pre-incubation CJ/NCL crystal diffraction of 3.0 Å. Intriguingly however, while GA cross-linking did not overtly disrupt CJ-LPC crystal quality when observed on a macroscopic level via stereomicroscopy, it did disrupt the molecular order as observed by XRD; GA cross-linked CJ-LPCs demonstrated markedly reduced pre-incubation molecular order—to the point that the XRD data could not be comparatively indexed and scaled. These results indicate the molecular order of CJ/OA and CJ/EDC crystals was maintained throughout the cross-linking method, while GA cross-linked crystals became more disordered. Conversely, GA was the only cross-linking agent capable of stabilizing tetragonal HEWL crystals, both on a macroscopic level, as seen by stereomicroscopy, and on a molecular level, yielding a post-cross-linking diffraction resolution of 2.0 Å. The same cross-linked crystals were subsequently subjected to HDFa cell culture for 24 hours after which the post-incubation retention of molecular order was measured again using XRD. All cross-linked CJ-LPCs as well as the HEWL/GA crystals exhibited post-incubation resolution comparable to their respective pre-incubation resolution estimates (Fig. 3 *Table*)—suggesting these cross-linked protein crystal materials can retain their molecular order in environments well outside their crystallization condition and in the presence of HDFa cells.

Potential cytotoxic effects from GA, OA, or EDC cross-linking was investigated by measuring the viability of HDFa and human macrophage (MV-4-11) cells when subjected to cross-linked protein crystal materials. Prior to cross-linking and incubation with human cells, large CJ-LPCs and HEWL crystals were first fragmented by sonication to increase their surface area and thereby maximize the potential cytotoxic response[20] (Supporting Information). The particle size distribution of fragmented CJ-LPCs was observed via scanning electron microscopy (SEM). SEM images were processed using image stitching and particle detection packages in Fiji[21,22] and quantified via histogram plotting tools in MATLAB version 9.1.0 (Natick, MA). The mean particle size was found to be 5.8 ± 3.9 µm with a mode of about 3.3 µm (Fig. S1).

To prepare for incubation with HDFa cell culture, cross-linked fragmented protein crystal materials were sterilized in high-salt buffers containing 20% ethanol, washed in sterile PBS pH 7.5, and transferred to sterile supplemented cell culture medium (Supporting Information). HDFa cells were plated at a density of 150,000 cells/mL within a 96 well plate and allowed to adhere for 24 hours. After the initial 24-hour period, the old medium was evacuated and replaced with new supplemented medium containing the various fragmented protein crystal materials in a range of concentrations (1, 50, 100, 200, and 400 µg/mL) determined by Bradford

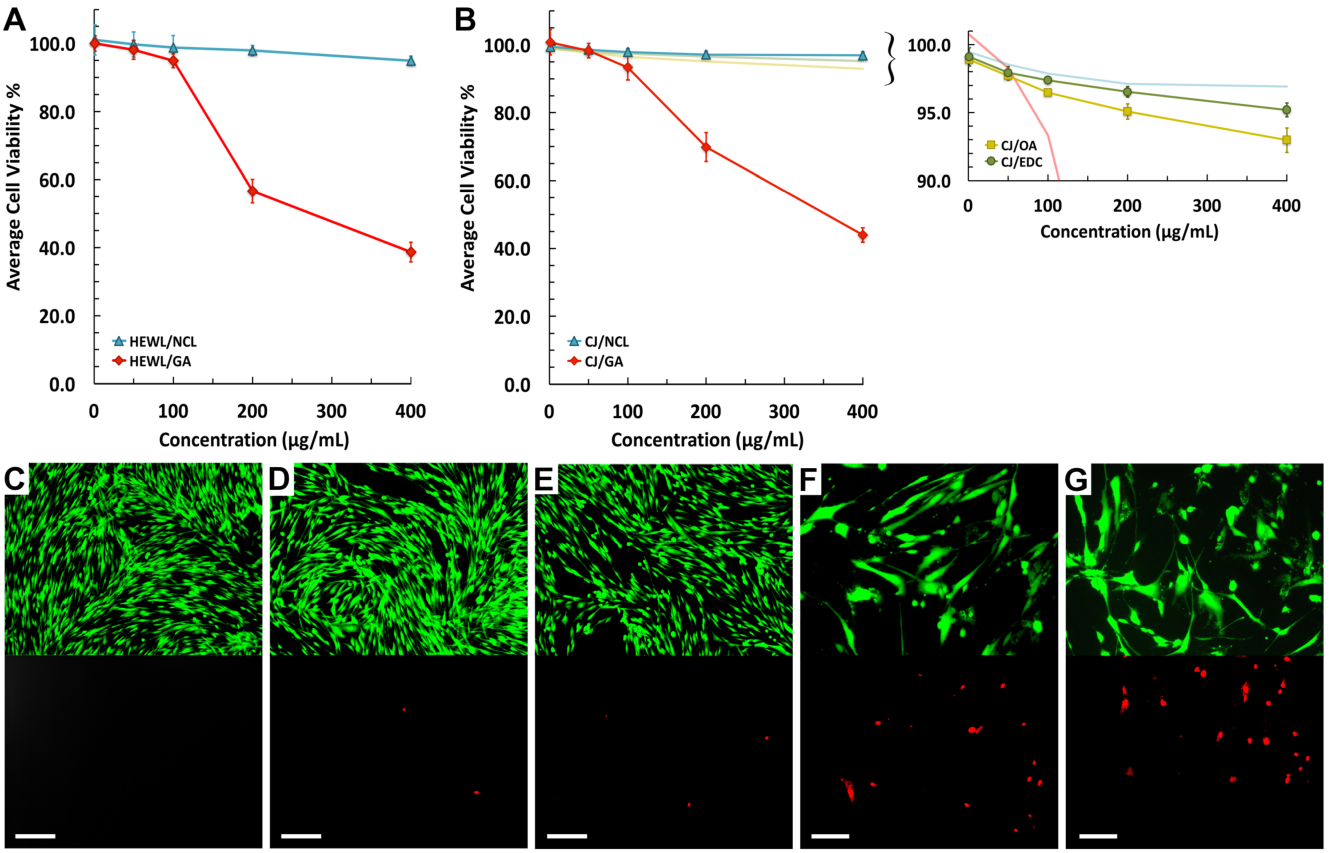

Figure 4. (A) HDFa cell viability under varying concentrations of fragmented HEWL protein crystal materials; *Error Bars:* standard deviation, n=3. (B) HDFa cell viability under varying concentrations of fragmented CJ-LPC materials; *Error Bars:* standard deviation, n=3. (C) Control HDFa cells with no material added to the medium; *Scale Bar:* 300 µm; *Top:* green fluorescent live cell stain (calcein); *Bottom:* red fluorescent dead cell stain (ethidium homodimer). (D) HDFa cells incubated with 400 µg/mL CJ/EDC; *Scale Bar:* 300 µm. (E) HDFa cells incubated with 400 µg/mL CJ/OA; *Scale Bar:* 300 µm. (F) HDFa cells incubated with 400 µg/mL CJ/GA; *Scale Bar:* 100 µm. (G) HDFa cells incubated with 400 µg/mL HEWL/GA; *Scale Bar:* 100 µm.

assay. Cells were incubated in the presence of protein crystal materials for an additional 24 hours, after which, cell viability was measured using the Pierce™ lactate dehydrogenase (LDH) cytotoxicity assay kit (Fig. 4A & 4B). While HEWL/NCL sample wells maintained very high cell viability across all concentrations, HEWL/GA materials prompted a precipitous decline in cell viability corresponding to increasing material concentration—suggesting a toxic response to GA. Similarly, CJ/GA materials also triggered a dramatic decrease in cell viability corresponding to increasing material concetration. Conversely, CJ/OA, CJ/EDC, and CJ/NCL materials preserved cell viability despite high material concentrations (up to 400 μg/mL). We suspect the slightly diminished viability seen in CJ/NCL sample wells compared to HEWL/NCL samples is due to trace quantities of endotoxin, which is progressively removed during CJ-LPC material purification, crystallization, and subsequent wash steps (Fig. S3). The more pronounced reduction in cell viability for GA cross-linked crystals can likely be attributed to unreacted GA that has leached from the crystals into the growth medium.

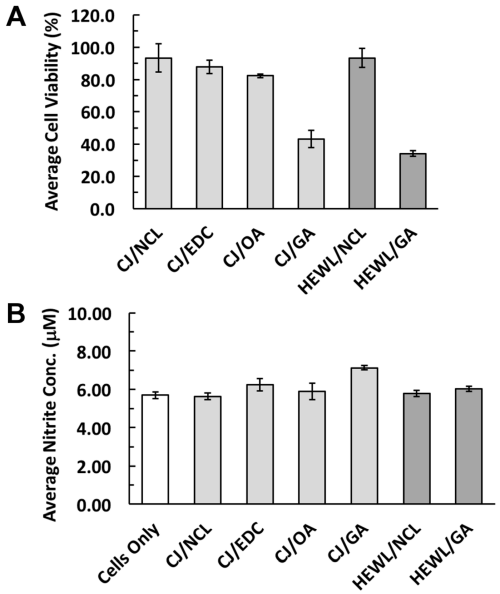

Figure 5. (A) MV-4-11 cell viability when incubated with various protein crystal materials at a concentration of 400 μg/mL; *Error Bars:* standard deviation, n=3. (B) Nitrite concentration released from MV-4-11 cells incubated with 400 μg/mL of various protein crystal materials.; *Error Bars:* standard deviation, n=3.

The HDFa viability quantified by LDH activity was qualitatively confirmed by live/dead staining (Fig. 4C-4G); calcein (green) was used as the live cell stain while dead cells were visualized using ethidium homodimer (red). Control cells, not subjected to any materials, were compared to cells incubated with 400 μg/mL of various cross-linked protein crystal materials. The cell counts for control cells as well as cells incubated with CJ/EDC and CJ/OA crystals show minimal cell death, while cells incubated with CJ/GA and HEWL/GA materials appear to suffer approximately 50% cell death. These images agree with quantitative data from the LDH assay—indicating minimal loss of cell viability for EDC and OA cross-linked protein crystal materials and a much higher loss of viability for protein crystal materials cross-linked by GA. More details concerning the LDH, endotoxin, and live/dead staining assays can be found in the Supporting Information.

To prepare for incubation with MV-4-11 cell culture, cross-linked fragmented protein crystal materials were sterilized in high-salt buffers containing 20% ethanol, washed in sterile PBS pH 7.5, and transferred to sterile double deionized water (Supporting Information). Fragmented crystal materials were transferred to an empty 96-well plate at a concentration of 400 μg/mL and allowed to dry overnight. MV-4-11 cell suspension was then added to the dried material at a density of 150,000 cells/mL. Cells were then incubated in the presence of the fragmented protein crystal materials for 24 hours, after which the cell viability (Fig. 5A) and nitrite concentration was determined (Fig. 5B). The viability trend for MV-4-11 cultures is commensurate to HDFa cells, showing high viability for both NCL crystals as well as OA and EDC cross-linked protein crystal materials, while both CJ/GA and HEWL/GA materials engendered low cell viability. All samples tested demonstrated low nitrite concentration relative to the negative control (cells only), indicating these materials do not appear to promote human macrophage activation.

CONCLUSION

A priori it was not known if chemically modifying CJ-LPC interfaces would substantially degrade diffraction quality. While GA, the cross-linking agent primarily used to stabilize protein crystals, generated robust CJ-LPCs on a macroscopic level when tested against HDFa cell culture, it exhibited the greatest initial loss in molecular order upon cross-linking. Migneault et al. details the complex solution properties of GA and lists 13 proposed forms ranging from monomeric to highly polymerized.[23] Thus, in this case, the heterogeneous nature of GA is likely at odds with preserving molecular order at the lysine rich interfaces of CJ-LPCs. Surprisingly, the seldom used cross-linkers, OA and EDC, generated CJ-LPC materials capable of retaining molecular order post-incubation while suffering minimal loss of diffraction upon cross-linking.

Conversely, cross-linking tetragonal HEWL with GA was shown to be effective at both stabilizing the crystal and preserving diffraction quality; these results support previous findings.[24] To date, neither OA nor EDC has been effective at stabilizing HEWL crystals. This is not surprising considering the small number of amines at HEWL crystal interfaces as well as a lack of proximal amine to carboxylic acid pairs at crystal interfaces. OA is the shortest dialdehyde and primarily monomeric, which may limit its ability to be effective.[25] In this case, the ability to polymerize may enable GA to sufficiently cross-link HEWL crystals.

The results of the stability and toxicity tests suggest that both OA and EDC cross-linked CJ-LPC materials are superior to protein crystals cross-linked by GA, demonstrating both promising molecular stability and cytocompatibility when tested in the short-term against HDFa and MV-4-11 cells. These materials may be particularly well suited for use in biocatalysis, drug delivery, biosensing, and environmental remediation. Further genotoxicity, and immunogenicity studies should be done to determine long-term biocompatibility toward a more diverse set of tissue types. By pursuing this research, we hope to better understand protein crystal materials and leverage that knowledge to design advanced nanostructured devices for applications in biotechnology and nanomedicine.

AUTHOR INFORMATION

Corresponding Author

* Email: Christopher.Snow@ColoState.edu

Author Contributions

L.F.H., H.T.B., S.P.J., and C.D.S. conceived of the experiments; L.F.H. and C.D.S. wrote the manuscript; L.F.H. expressed and purified the protein, and performed XRD, SEM, endotoxin and nitrite analyses; L.F.H. and D.A.A. grew and cross-linked the crystals aided by methods developed by T.R.H.; finally, L.F.H. and H.T.B. maintained the cell cultures and performed the LDH assay, live/dead staining, and all microscopy imaging.

ACKNOWLEDGMENTS

The authors would like to thank Morgan Hawker for her aid in SEM training, Aidan Friederich for assistance with the LDH cytotoxicity assay, and finally Matt Kipper, Ellen Fisher, and Ketul Popat for thoughtful discussion. This research was supported in part by the Compatible Polymer Network project funded by the Colorado State University Office of the Vice President for Research and by the National Science Foundation grant number 1506219. The authors declare no competing financial interest.

SUPPORTING INFORMATION

Electronic supporting information includes reagent list and protein/DNA sequences, as well as methods and data pertaining to: protein expression, purification and crystallization, crystal fragmentation, SEM imaging, human cell culture, XRD data collection, indexing, and scaling, stereomicroscopy, endotoxin quantification, LDH cytotoxicity, nitrite detection, and live/dead staining.

REFERENCES

(1) Margolin, A. L.; Navia, M. A. Protein Crystals as Novel Catalytic Materials. *Angew. Chem. Int. Ed.* **2001**, *40* (12), 2204–2222. DOI: 10.1002/1521-3773(20010618)40:12<2204::AID-ANIE2204>3.0.CO;2-J

(2) Noritomi, H.; Koyama, K.; Kato, S.; Nagahama, K. Increased Thermostability of Cross-Linked Enzyme Crystals of Subtilisin in Organic Solvents. *Biotechnol. Tech.* *12* (6), 467–469. DOI: 10.1023/A:1008863407130

(3) Lee, T. S.; Turner, M. K.; Lye, G. J. Mechanical Stability of Immobilized Biocatalysts (CLECs) in Dilute Agitated Suspensions. *Biotechnol. Prog.* **2002**, *18* (1), 43–50. DOI: 10.1021/bp010131j

(4) Ayala, M.; Horjales, E.; Pickard, M. A.; Vazquez-Duhalt, R. Cross-Linked Crystals of Chloroperoxidase. *Biochem. Biophys. Res. Commun.* **2002**, *295* (4), 828–831. DOI: 10.1016/s0006-291x(02)00766-0

(5) Yan, E. K.; Cao, H. L.; Zhang, C. Y.; Lu, Q. Q.; Ye, Y. J.; He, J.; Huang, L. J.; Yin, D. C. Cross-Linked Protein Crystals by Glutaraldehyde and Their Applications. *RSC Adv.* **2015**, *5* (33), 26163–26174. DOI: 10.1039/c5ra01722j

(6) Basu, S. K.; Govardhan, C. P.; Jung, C. W.; Margolin, A. L. Protein Crystals for the Delivery of Biopharmaceuticals. *Expert Opin. Biol. Ther.* **2004**, *4* (3), 301–317. DOI: 10.1517/eobt.4.3.301.27331

(7) Zhang, Y.; Chan, H. F.; Leong, K. W. Advanced Materials and Processing for Drug Delivery: The Past and the Future. *Adv. Drug Deliv. Rev.* **2013**, *65* (1), 104–120. DOI: 10.1016/j.addr.2012.10.003

(8) Clair, N. S.; Shenoy, B.; Jacob, L. D.; Margolin, A. L. Cross-Linked Protein Crystals for Vaccine Delivery. *Proc. Natl. Acad. Sci.* **1999**, *96* (17), 9469–9474. DOI: 10.1073/pnas.96.17.9469

(9) Hoskin, F. C.; Walker, J. E.; Stote, R. Degradation of Nerve Gases by CLECS and Cells: Kinetics of Heterogenous Systems. *Chem. Biol. Interact.* **1999**, *119–120*, 439–444. DOI: 10.1016/s0009-2797(99)00056-3

(10) Luiz de Mattos, I.; Lukachova, L. V.; Gorton, L.; Laurell, T.; Karyakin, A. A. Evaluation of Glucose Biosensors Based on Prussian Blue and Lyophilised, Crystalline and Cross-Linked Glucose Oxidases (CLEC(R)). *Talanta* **2001**, *54* (5), 963–974. DOI: 10.1016/s0039-9140(01)00367-8

(11) Roy, J. J.; Abraham, T. E.; Abhijith, K. S.; Kumar, P. V. S.; Thakur, M. S. Biosensor for the Determination of Phenols Based on Cross-Linked Enzyme Crystals (CLEC) of Laccase. *Biosens. Bioelectron.* **2005**, *21* (1), 206–211. DOI: 10.1016/j.bios.2004.08.024

(12) Laothanachareon, T.; Champreda, V.; Sritongkham, P.; Somasundrum, M.; Surareungchai, W. Cross-Linked Enzyme Crystals of Organophosphate Hydrolase for Electrochemical Detection of Organophosphorus Compounds. *World J. Microbiol. Biotechnol.* **2008**, *24* (12), 3049–3055.
DOI: 10.1007/s11274-008-9851-y

(13) Speer, D. P.; Chvapil, M.; Eskelson, C. D.; Ulreich, J. Biological Effects of Residual Glutaraldehyde in Glutaraldehyde-Tanned Collagen Biomaterials. *J. Biomed. Mater. Res.* **1980**, *14* (6), 753–764. DOI: 10.1002/jbm.820140607

(14) Amri, M. A.; Firdaus, M. a. B.; Fauzi, M. B.; Chowdhury, S. R.; Fadilah, N. R.; Wan Hamirul, W. K.; Reusmaazran, M. Y.; Aminuddin, B. S.; Ruszymah, B. H. I. Cytotoxic Evaluation of Biomechanically Improved Crosslinked Ovine Collagen on Human Dermal Fibroblasts. *Biomed. Mater. Eng.* **2014**, *24* (4), 1715–1724. DOI: 10.3233/BME-140983

(15) Niknejad, H.; Mahmoudzadeh, R. Comparison of Different Crosslinking Methods for Preparation of Docetaxel-Loaded Albumin Nanoparticles. *Iran. J. Pharm. Res. IJPR* **2015**, *14* (2), 385–394. PMID: 25901145

(16) Kowalski, A. E.; Huber, T. R.; Ni, T. W.; Hartje, L. F.; Appel, K. L.; Yost, J. W.; Ackerson, C. J.; Snow, C. D. Gold Nanoparticle Capture within Protein Crystal Scaffolds. *Nanoscale* **2016**, *8* (25), 12693–12696. DOI: 10.1039/c6nr03096c

(17) Huber, T. R.; Hartje, L. F.; McPherson, E. C.; Kowalski, A. E.; Snow, C. D. Programmed Assembly of Host–Guest Protein Crystals. *Small* **2017**, *13*, 1602703.
DOI: 10.1002/smll.201602703

(18) Hartje, L. F.; Munsky, B.; Ni, T. W.; Ackerson, C. J.; Snow, C. D. Adsorption-Coupled Diffusion of Gold Nanoclusters within a Large-Pore Protein Crystal Scaffold. *J. Phys. Chem. B* **2017**, *121* (32), 7652–7659. DOI: 10.1021/acs.jpcb.7b03999

(19) Hekmat, D.; Hebel, D.; Schmid, H.; Weuster-Botz, D. Crystallization of Lysozyme: From Vapor Diffusion Experiments to Batch Crystallization in Agitated Ml-Scale Vessels. *Process Biochem.* **2007**, *42* (12), 1649–1654. DOI: 10.1016/j.procbio.2007.10.001

(20) Ducheyne, P.; Healy, K.; Hutmacher, D. E.; Grainger, D. W.; Kirkpatrick, C. J. Comprehensive Biomaterials; *Elsevier*, 2011. DOI: 10.1016/c2009-1-28384-5

(21) Preibisch, S.; Saalfeld, S.; Tomancak, P. Globally Optimal Stitching of Tiled 3D Microscopic Image Acquisitions. *Bioinformatics* **2009**, *25* (11), 1463–1465. DOI: 10.1093/bioinformatics/btp184

(22) Schindelin, J.; Arganda-Carreras, I.; Frise, E.; Kaynig, V.; Longair, M.; Pietzsch, T.; Preibisch, S.; Rueden, C.; Saalfeld, S.; Schmid, B.; et al. Fiji: An Open-Source Platform for Biological-Image Analysis. *Nat. Methods* **2012**, *9* (7), 676–682. DOI: 10.1038/nmeth.2019

(23) Migneault, I.; Dartiguenave, C.; Bertrand, M. J.; Waldron, K. C. Glutaraldehyde: Behavior in Aqueous Solution, Reaction with Proteins, and Application to Enzyme Crosslinking. *BioTechniques* **2004**, *37* (5), 790–796, 798–802. PMID: 15560135

(24) Wine, Y.; Cohen-Hadar, N.; Freeman, A.; Frolow, F. Elucidation of the Mechanism and End Products of Glutaraldehyde Crosslinking Reaction by X-Ray Structure Analysis. *Biotechnol. Bioeng.* **2007**, *98* (3), 711–718. DOI: 10.1002/bit.21459

(25) Whipple, E. B. Structure of Glyoxal in Water. *J. Am. Chem. Soc.* **1970**, *92* (24), 7183–7186. DOI: 10.1021/ja00727a027

Insert Table of Contents artwork here